FUDMA Journal of Renewable and Atomic Energy (FJoRAE)
ISSN: 3027-2335
Vol. 1 No 2, June 2024. Pp 92-123

https://doi.org/10.33003/fjorae.2024.0102.07

Robust LQR-Based Autopilot Design for Hybrid Energy Harvesting UAVs

O. C. Ubadike [1], G. E. Abbe[1],T. E. Amoako [1,], M. U. Bonet[1] , M.O. Momoh*[2], C. A. Adeboye[1], K. P. Ter[1]

[1] Department of Aerospace Engineering, Air Force Institute of Technology Kaduna, Nigeria.

[2] Department of Mechatronics Engineering, Air Force Institute of Technology Kaduna, Nigeria.

ABSTRACT

The hybrid energy harvest light surveillance unmanned aircraft is designed to be powered with a wind energy fuel-cell. The fuel-cell will produce electrical energy through a regenerative chemical reaction. In the absence of this chemical reaction, energy will be extracted from the vertical gradients of the horizontal wind through a process known as dynamic soaring. For the safe operation of the UAV, stabilization and trajectory control are essential. These features are achieved with the aid of a robust flight control system (autopilot). Owning to the advantages of Linear Quadratic Regulator (LQR) over other controllers which include, its ability to handle Multiple INpute Multiple Output systems and its superior performanc when handling unceertainties and disturbances, it was employed for the design of the control system. The nonlinear simulation model that gives a good representation of the UAV in MATLAB/Simulink environment was developed taking into account the aerodynamic components in 6DOF of equation of motion, the propulsion and the gravity effects. Trimming, decoupling and linearization of the developed nonlinear model were carried out. In order to evaluate the performance of the LQR controller, the response of the system to perturbation was compared to that of the closed loop system with the LQR implemented. In the open loop case none of the states being measured returned to their original value after the introduction of disturbances for 2 seconds. For the closed loop control using the LQR, stability was achieved in the following states; Side velocity, Yaw Rate, Yaw angle, Roll rate and roll angle with their settling times being 36, 40, 41, 30 and 46 seconds respectively. Open loop responses of the models to various control inputs indicated the accuracy of the models. The linearized models were used to design the Autopilot system that has the tendency of stabilizing the UAV in the presence of any uncertainty. The closed loop systems were tested and the influence of different disturbances and the results indicated that the LQR base autopilot is robust enough to ensure safe flight of the UAV

Keywords: Autopilot, LQR, Energy-Harvesting UAV, Decoupling, Linearization

INTRODUCTION

Over the years, Unmanned Aerial Vehicles (UAVs) have attracted the attention of scientists and engineers who have been working on the design and development in order to increase the autonomy and endurance of these vehicles (Mohsan et al., 2022). This has been amplified by concerted efforts towards environmentally benign vehicles and alternative renewable energy

* Corresponding Author's contact: momuyadeen@gmail.com

technology. The primary goal has been to enhance environmental benefits while expanding [1]mission range and endurance of UAVs. UAV endurance has only been limited due to mass and volume challenge for the storage of energy. UAV endurance is primarily constrained by fuel capacity due to the mass and volume challenge for the storage of energy. Therefore, innovative approaches have been considered with the view to enabling longer range and autonomy. Such innovation includes the use of energy from the surrounding environment like wind, solar or hybrids (Boukoberine & Zhou, 2019).

The UAVs have a wide range of applications mostly in military for reconnaissance, environmental observation, maritime surveillance and mine removal activities (Yao et al., 2019). They can also be used in non-military application such as aerial photography, surveillance, pipeline and utility line inspection and convoy escort (Chaturvedi et al., 2019). The use of autonomous vehicles (UAVs) by the Nigerian military has effectively provided solutions to several challenges in their operations, such as the resupply of medical stores in the battle field to prevent loss of lives, invasion of illegal immigrants through unsecured borders and search and rescue operation in the maritime domain. However, the operation of the autonomous vehicles has the limitation of mission range and endurance. The current internal security challenges in Nigeria have brought to the fore the need to design a hybrid energy harvest light surveillance unmanned aircraft to increase mission range and endurance. To tackle some of the operational challenges faced by the Nigerian military, the Air Force Institute of Technology (AFIT), Nigeria, has successfully designed and developed an Unmanned Aerial Vehicle (UAV) known as the 'AFIT Hybrid Energy-Harvesting UAV'. This innovative UAV is the outcome of the annual Group Design Project (GDP), a compulsory requirement for AFIT's M.Eng. program in Aerospace Engineering. The hybrid energy harvest light surveillance unmanned aircraft is conceptualized to embrace novel technologies for increased persistence during operations while having high survivability.

The hybrid energy harvest light surveillance unmanned aircraft is required to be powered with a wind energy and fuel-cell and has a mission take-off weight of 10 kg. The basic principle of the wind energy-harvesting fuel-cell powered UAV will be that, the fuel-cell pack within the airframe will produce electrical energy through a regenerative chemical reaction. In the absence of this chemical reaction, energy will be extracted from the vertical gradients of the horizontal wind through a process known as dynamic soaring. The power obtained is primarily used for propulsion and on-board electronics. The energy storage device will be charged with surplus power while the energy harvested from wind will be used to maintain flight through soaring. In the absence of wind, the energy storage device becomes the source of energy.

[1] *Corresponding Author's contact: momuyadeen@gmail.com

Autopilot system (Flight control system) guide UAVs during flight without any assistance of a pilot. It is an onboard intelligent system that ensure stabilization and trajectory control of the UAV and it consists of state sensors and controller. The state sensors continuously measure parameters of the UAV by using multiple sensors such as GPS, accelerometer, magnetometer, gyros and pitot-tube. The controller measures and calculates the error between current and required states. The autopilot system (Flight control system) as shown in the block diagram in Figure 1, makes use of the data obtained from the onboard sensor and radio transmitted digital commands received from a Ground Control Station (GCS), together with a control algorithm to compute adequate control signal (U) (O. C. Ubadike et al., 2022).

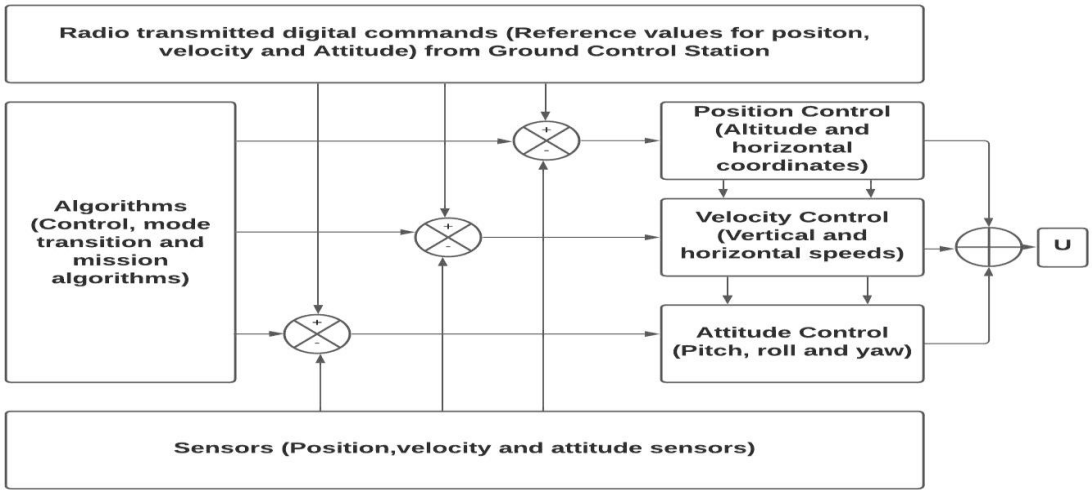

Figure 1: Flight Control loop of an aircraft [5].

The control signal actuates the control surfaces to ensure stabilization and trajectory control of the UAV. The Autopilot of Unmanned Aerial Vehicle (UAV) is a system that is able to control the attitude (roll, pitch, and yaw) of UAV. It also has the capability to maintain the altitude of UAV, aids UAV to travel according to the waypoints and take-off/landing automatically. Every detail of the autopilot system are to be carefully optimized with respect to weight, power consumption and capability during system development (Wahab et al., 2006).The remainder of this paper is organized as follows: Section 2 presents a review of some fundamental concepts as well as review of some related literature. Section 3 presents the materials and method employed. Section 4 and 5 presents the results obtained and conclusion respectively.

Aircraft motions are described through a set of first order nonlinear differential equation referred to as Equation of motion (EOM). EOM defines the rotational and translational velocities, derived using newton's second law motion. It also contains navigation and kinematic equations describing the aircraft's position and attitude respectively. It describes the system's response to

various inputs and states over time. Various methods are used to derive a system equation of motion based conservation of linear and momentum (Muraleedharan et al., 2020). The EOM contains the equations governing the translational and rotational motion of an aircraft which includes (Naser et al., 2016);

1. The kinematics equations defining the translational position and rotational positions relative to the earth reference.
2. Dynamic equation relating forces to translational acceleration and moments to rotational acceleration.
3. Equations defining the variable-mass characteristics of the airplane (center of gravity, mass and moments of inertia) versus time.
4. Equations giving the positions of control surfaces and other movable parts of the airplane (landing gear, flaps, wing sweep, etc.) versus time

Dynamic models can either be represented in a form of differential equations or systems of linear equations. These equations capture the variability and process of system states over time and changing inputs (Muraleedharan et al., 2020). It includes deriving the nonlinear equations of motion (translational and rotational equations) for the UAV, considering the external forces and moment acting on the body due to aerodynamics, gravity and propulsion. The linearization and decoupling of the equations of motion to create a reduced order transfer-function and state-space models appropriate for control design (Kumar, 2015). Various techniques are used to develop dynamic models for UAVs. Many have been derived from methods employed for modelling rigid bodies, manned aircraft and robotic systems (Muraleedharan et al., 2020). The most common method used for modelling of conventional fixed wing UAV is the Newton–Euler methods, which are based on the core concept of Newton's second law.

The Newton–Euler method is based on the general frame work of the Newton equation of motion for translational motion and the Euler equation for rotational motion to obtain the mathematical modeling of the nonlinear equations of motion (Kumar, 2015). Ryll et al, modelled a quadrotor with tilting propellers (holocopter) by analyzing quadrotor which was considered in the paper as a connection of five main rigid bodies in relative motion among themselves: the four propeller groups and the quadrotor body itself (Ryll et al., 2014). By Newton–Euler procedure, a complete description of the quadrotor dynamic model was derived by considering the forces/moments generated by the motion of the propeller, as well as any cross coupling due to gyroscopic and inertial effects arising from the relative motion of the five bodies composing the quadrotor (Ryll et al., 2014). Additionally, with the aid of the model, a dynamic output linearization technique was designed for trajectory control of the UAV.

Ea et al., 2015, also applied this method to obtain the mathematical model of the non linear equation of motion by capturing the dynamics and kinematics of the Ultrastick -25 fixed wing UAV. The non-linear equation was decomposed and linearised into lateral and longitudinal mode. The behaviour of the state non linear UAV was compared to the resulted linear model by applying doublet signals in the control surface to check the matching between them (Ahmed et al., 2015). Furthermore in authors in (Srour et al., 2021), presented the mathematical modeling of a Fixed-Wing Unmanned Aircraft Vehicle (UAV) which is a Delta-Wing. Newton Euler formulas were used for both lateral and longitudinal axes to obtain the model. The simulations on the XFLR5 software produce the aircraft's characteristics from aerodynamic coefficients, inertias, and operating regions in a way that is consistent with the prototype.

Euler-Lagrange approach is another method for modelling UAV, it does not require a particular identification of the coordinate system but makes use of the conservation of energy to derive the equation of motion (Saeed et al., 2015). A survey conducted by (Saeed et al., 2015) revealed that the Euler-Lagrange method have only been used in few research works for the modelling without stating reasons for their selection. (Escareno et al., 2006) developed the mathematical model of the aircraft's altitude in vertical mode through the Euler-Lagrange method. Also, (Hussain et al., 2018) empolyed the method to derive the equation of motion and numerical simulation of a passive robotic walker. More so authors in (Martini et al., 2022), derived the mathematical model for quadrotor UAVs using the Euler-Lagrange formulation.

Considering the aerodynamic forces and moments of a fixed wing UAV, there are different methods which can be used to model the forces and moment acting on the UAV. These methods include, wind tunnel analysis, computational fluid dynamics, aerodynamic equations and system identification as stated in (Muraleedharan et al., 2020). The wind tunnel analysis is very expensive and obtaining useful data is very time consuming hence makes it unpracticable for low-cost UAVs (Simmons, 2018). Using the computational fluid dynamics to developing accurate estimates for all parameters needed for modelling UAV may be difficult. Therefore, the most common method for modelling fixed wing UAV that provide useful flight dynamics without any challenge is the system identification (Simmons, 2018).

System identification is usually done on a certain parameterized model defined by the user with knowledge of the physical equations governing flight (Khan & Nahon, 2013). It is the most recent approach to modelling the aerodynamic behavior of fixed-wing aircraft and entails developing a mathematical models based on estimates, general models, and then using data collected from flight to fit the models (Muraleedharan et al., 2020). Based on the aerodynamic analysis, multi-input, multi-output underactuated linear model configuration was deduced by (Liu et al., 2015). Utilizing the real-time flight data collected from human-controlled test flight, a two-input three-output linear model was obtained by means of system identification. Authors in

(Qazi et al., 2017), modelled a UAV longitudinal dynamic through system identification method. The project aimed at system identification of a fixed wing UAV by means of specifically designed flight experiment. The flight maneuvers designed were performed on the UAV and aircraft states and recorded during the flight. The data obtained were preprocessed for noise filtering and bias removal followed by parameter estimation of the longitudinal dynamics transfer function using MATLAB system identification.

Control laws

In order to ensure that the UAV delivers its desired performance and accurately follows the desired path in the presence of wind and other external distance, a control algorithm which is the critical part of the Flight Control System must be developed. Once the longitudinal and lateral instabilities are established, the instabilities must be addressed to achieve an autonomous flight hence the need for a robust controller. Previous literatures on flight control system, reviewed most autopilots for UAVs are Proportional Integral Derivative (PID) controllers due to their reliability, simplicity in structure and ease to design. Recently, PID-based controllers have been applied successfully by different researchers. The dynamic behavior of the aircraft was analyzed and five PID controllers in three loops were designed based on the root-locus techniques [20]. In addition authors in (Oktay et al., 2016), carried out a research on how to increase flight performance of small unmanned aerial vehicle (ZANKA-I) using an autopilot system having a PID -based hierarchical control structure. (Mazlan et al., 2021), utilised PID controllers to design an automatic flight control system for fixed wing UAV using X-Plane and LabVIEW

However, the performance of the PID controllers is limited due to the presence of nonlinearity, time varying parameters and disturbance (Abubakar et al., 2019; Chao et al., 2007). It does not account for the cross-coupling effects of UAVs since it is applicable to only Single Input Single Output (SISO) system (Saeed et al., 2015). To overcome these challenges, a more robust and adaptive controllers such as Linear Quadratic Regulator, Neutral Network, sliding mode, Lead-Lag, Fuzzy Logic and state feedback controllers would be required (Sanusi et al., 2022).

The authors in (Hamissi et al., 2019), investigated problems of robust flight control system for a fixed wing aircraft and stated that such systems are of Multi-Input Multi-Output (MIMO) form, tightly coupled and nonlinear. They proposed a Combined Homogeneous High Order Sliding Mode (HHOSM) and Nonlinear Dynamic Inversion (NDI) approaches to deal with the piloting controller. The complete controller was designed to ensure the tracking of desired attitude angles and longitudinal velocity. The Nonlinear Dynamic Inversion (NDI) used the nonlinear full state feedback to linearize the dynamics of controlled variable selected and the linear controller was applied to regulate these variables with a desirable closed loop behavior. The nonlinearity was handled by Homogeneous High Order Sliding Mode controller. The results obtained after

simulation on real time virtual simulation for the development of aircraft control system demonstrated that HHOSM-NDI control system delivers a high dynamic tracking performance and also alleviate the chattering effect. Even though Sliding Mode Control (SMC) is an effective controller that deals with uncertainties and external disturbances in nonlinear dynamic system, it has some shortcomings. This is due to the fact that it is restricted to systems having relative degree equal to one and yields a well-known chattering effect(a phenomenon of high frequency and finite amplitude oscillations that degrades the performance) (Hamissi et al., 2019). In overcoming this challenge, HHOSMC was employed to maintain the robustness properties of a standard SMC and also alleviate the chattering effects.

Control system that employs NDI of the aircraft model improve performance level over linear flight control design without requiring gain scheduling. The NDI is to cancel the non-linear dynamics so the system can be controlled as a linear system hence, requires much information about the system else the required output might not be achieved. However, the problem with NDI is that the mathematical model of the system is often very complex which makes the controller complex (Karlsson, 2002).

In (Salman & Anavatti, 2012), applied fuzzy model-based controller with new analytical inversion method for attitude control problem of UAV. (Guo et al., 2022), developed a control algorithm by combining fuzzy adaptive control and sliding mode variable structure control to overcome the complexity of the coupled nonlinear model of a fixed-wing UAV and the uncertainty caused by a large number of interference factors. The control algorithm was mainly based on the sliding mode variable structure, which dealt with the problem of the strongly coupled complex nonlinear system. Due to the chattering effects of sliding mode controller, a fuzzy adaptive control method was introduced to reduce the chattering problem and also approximate the uncertain parameters and unknown functions caused by external disturbance. The results showed that the method had a fast response speed, small steady-state error and strong robustness. For these reasons, it was recommended for complicated, nonlinear, strongly coupled and multiple uncertainties models such as multiple-rotors UAV models. Even though fuzzy controllers can be applied to nonlinear systems, their stability and robustness are tedious to prove analytically.

From the industrial perspective, recently, FCS laws employ multivariable techniques blended with classical tools. Linear Quadratic Regulator (LQR) and Nonlinear Diversion Inversion (NDI) are the most successful multivariable methods (Karakaş, 2007). The first significant applications of multivariable control techniques started at Boeing in 1978 as part of a research program and the results demonstrated that multivariable control law design techniques offered significant advantages over classical techniques in the solution to multi-loop control problems (Balas, 2003). Since then, Boeing has successful applied multivariable control combined with classical control to a number of aircraft.

LOR is very robust when considering uncertainties in the system model and also determines the all the gains in MIMO system controller simultaneously (Mohammed et al., 2022; O. Ubadike et al., 2022). Owing to the advantages of LQR; overcoming the big disturbance which affect the stability of a system without reducing the performance of the system, LQR controller was used by (Purnawan & Purwanto, 2017) to design a control system for LSU-05 to ensure its stability.

Authors in (Kanokmedhakul et al., 2019), also presented on the use of differential evolution for tuning a PID controller, LQR with an integral action for aircraft pitch controller. The performance of the controllers was investigated based on single step and multiple steps response while some disturbances were introduced. The results indicated that PID controller was efficient for response speed while the LOR with integral action was efficient for steady state error elimination, hence both controllers are robust and can handle disturbance rejections.

A simple controller using linear feedback and LQR to control the lateral dynamics of an aircraft was designed by (Ashraf et al., 2018). The response of these controllers were analyzed to identify which controller gave better performance. The results depicted that for different initial values of state space vectors both controllers had the ability to control the lateral parameters of aircraft but the setting time of the LQR was a little higher than linear feedback. Also, the maximum peak value of the LQR was less than that of the linear feedback. Thus, LQR gave good performance and great robustness against external disturbance with a slow transient response.

From the review, it was realized that many research works have been done on the modelling dynamics and control design approaches for Fixed Wing aircrafts. The various problems related to modelling methods and several controllersd were indentified. However, this thesis employed a LQR controllers owing to its robustness, good stability margin and overcoming huge disturbances without reducing working performance (Ashraf et al., 2018).

Dynamic Soaring

There has been a lot of research works conducted to find ways on improving the endurance of these UAVs but this project will focus on dynamic soaring. In order to improve the endurance, researchers have tried to exploit the concept of dynamic soaring technique of an Albatross and apply this to UAVs (Mir et al., 2021). The Albatross bird exploits this special maneuvering technique while flying in wind shear. Dynamic soaring is the extraction of energy from the air through velocity gradients (typically occurs close to the ground due to the boundary layer) or shear layers (happens typically on the leeward sides of mountains and ridges). To apply dynamic soaring to UAVs; the energy-harvesting mechanism, UAV parameters and wind field must be modelled (Wang et al., 2022). The model of the energy-harvesting mechanism will indicate the real time energy change during dynamic soaring and it will be based on the equation of motion and mechanical energy equation. [39] built this model under the non-inertial reference frame

using three axes' systems; the North-East-Down, the body and the wind axes systems as well as forces acting on the UAV. UAVs can conserve energy by making use of the wind gradients, thus extracting energy from the wind shear to sustain the flight. Therefore, the minimum wind shear is a crucial parameter, as dynamic soaring cannot be achieved without the presence of the required wind shear. Also, the electrical battery on the UAV has to take over as the primary power supply in the absence of wind shear. The wind field is vital in performing soaring flight, therefore, a well-defined model describing the wind dynamics would be required for the design of the controls to enable the UAV perform dynamic soaring flight. Wind shear is the difference in wind speed and direction over a relatively short distance in the atmosphere. The wind speed increases with altitude before reaching the free air stream value. Therefore, the wind field model can be estimated or approximated using linear model or nonlinear model.

The linear wind model is the simplest model for wind estimation in which the wind shear slope is constant with altitude (Akhtar et al., 2009). The nonlinear exponential model normally represents the wind shear velocity over sea and ridges and the wind shear speed increases exponentially before reaching the free air stream value (Momoh et al., 2022; Sachs, 2005). The nonlinear logarithmic model is usually use in meteorological studies and mostly applicable to measurement near the surface of the earth (Liu et al., 2015; Momoh et al., 2021). The exponential wind field is the closest to the real situation as compared to the linear and the logarithmic wind field model. Hence it was used by Wang et al., 2022 to model the wind field during their research on the modelling and application of dynamic soaring by UAVs.

MATERIALS AND METHODS

This section discusses the various method that was used in designing the autopilot system for the hybrid energy-harvesting UAV. These include the simulation platform that was used for the development, the modelling approaches adopted for the UAV dynamics; the control law utilized for the lateral and longitudinal motion control of the aircraft.

Simulation Platform

The coding of the mathematical model to give a representation of the UAV dynamics was done, using the MATLAB/Simulink software. Also, the platform was used to simulate the open loop responses of the model to various input. Furthermore, the autopilot control loops were done with the aid of the simulation platform.

Modelling

To fully represent the dynamics of the hybrid energy-harvesting UAV, the fixed wing UAV model was first developed by adopting the nonlinear 6DOF flat-earth equation of motion for a

rigid body using the Newton Euler method. The equation of motion was derived from Newton's second law of motion; which models the external forces and moments acting on the aircraft and the Euler's Kinematical representation, which depicted the attitude of the aircraft as shown in equation 1. The equation derived was modified to suit the dynamics of the hybrid energy harvest UAV by using data that was obtained from the conceptual design, experimental simulations (use to obtain aerodynamic information) and survey conducted on relevant literatures.

$$f(X,U) = \begin{bmatrix} \frac{1}{m}F^b - \omega_{b/e} \times V^b \\ I_b^{-1}\left(M^b - \omega_{b/e}^b X I_b \omega_{b/e}^b\right) \\ \text{H}\,(\phi)\omega_{b/e}^b \\ T_{e/b} V^b \end{bmatrix} \text{.......................................(1)}$$

Where; X is the state vector, f is the external forces vector, ω is the angular velocity vector, V is the linear velocity vector, I is the inertia matrix, M is the external moment vector, H is the angular momentum vector and T represent the transformation matrix. The subscripts and superscripts e and b represents the earth and body frames respectively. The mathematical model was developed in the body frame.

The following steps were taken to modify the equation (1) to suit the dynamics of the hybrid energy-harvesting UAV;

i. *Define the intermediate variables*
ii. *Set control limits on the control input vectors*
iii. *Modelling the Dimensionless Aerodynamic Force Coefficients in the Stability Frame*
iv. *Dimensionalization of Aerodynamic Forces in the Body Frame*
v. *Modelling Dimensionless Aerodynamic Moment Coefficients about Aerodynamic Center in the Body Frame*
vi. *Dimensionalization of Aerodynamic Moments about Aerodynamic Center in the Body Frame*
vii. *Computation of Aerodynamic Moments about Center of Gravity in the Body Frame*
viii. *Modelling the Propulsion effect*
ix. *Modelling the Gravity Effect*
x. *Representation of Model in Explicit First-order Form*

Define the intermediate variables

This step ensures that all the relevant variables used in designing the model are only a function of the state and control inputs given in equation (1). The 12 state inputs that represent the UAV and the control inputs vectors are as define in equation (2) and (3) respectively.

$$X = \begin{bmatrix} u \\ v \\ w \\ p \\ q \\ r \\ \phi \\ \theta \\ \psi \\ x \\ y \\ z \end{bmatrix} = \begin{bmatrix} X_1 \\ X_2 \\ X_3 \\ X_4 \\ X_5 \\ X_6 \\ X_7 \\ X_8 \\ X_9 \\ X_{10} \\ X_{11} \\ X_{12} \end{bmatrix} = \begin{bmatrix} \text{Forward Velocity,} \\ \text{Side Velocity} \\ \text{Vertical velocity} \\ \text{Roll Rate} \\ \text{Pitch Rate} \\ \text{Yaw Rate} \\ \text{Euler Roll Angle} \\ \text{Euler Pitch Angle} \\ \text{Euler Yaw Angle} \\ \text{x-direction} \\ \text{y-direction} \\ \text{z-direction} \end{bmatrix}$$

.....(2)

$$\bar{U} = \begin{bmatrix} U_1 \\ U_2 \\ U_3 \\ U_4 \end{bmatrix} = \begin{bmatrix} \text{Rolling motion control input} \\ \text{Pitching motion control input} \\ \text{Yawing motion control input} \\ \text{Propoulsion control input} \end{bmatrix} \quad \text{.....(3)}$$

All the variables relevant for the design of the model are represented in a form of these states and control inputs.

Table 1: Definition of some variables

S/N	Variables	Formulae
1	Airspeed, V_A	$\sqrt{u^2+v^2+w^2}=\sqrt{x_1^2+x_2^2+x_3^2}$
2	Angle of attack, α	$tan^{-1}\left(\frac{\omega}{u}\right) = tan^{-1}\left(\frac{x_3}{x_1}\right)$
3	Angle of slip, β	$sin^{-1}\left(\frac{v}{v_R}\right) = sin^{-1}\left(\frac{x_2}{x_1^2+x_2^2+x_3^2}\right)$
4	Dynamic Pressure, Q	$^1/_2\,\rho V_A^2 =$ $0.5\times 1\cdot 225\times\left(\sqrt{x_1^2+x_2^2+x_3^2}\right)^2$ $= 0.6125\times(x_1^2+x_2^2+x_3^2)$
5	Angular velocity vector, $\omega_{b/_e}=\begin{pmatrix}p\\q\\r\end{pmatrix}$	$\begin{pmatrix}x_4\\x_5\\x_6\end{pmatrix}$
6	Translational velocity vector, $\bar{v}b=\begin{pmatrix}u\\v\\w\end{pmatrix}$	$\begin{pmatrix}x_1\\x_2\\x_3\end{pmatrix}$

Set control limits on the control input vectors

The controls employed on the hybrid energy-harvesting UAV are the aileron, elevator, rudder and throttle. Limits were specified to keep the UAV within a controllable flight envelop. The upper and lower control limits are as defined in Table 2.

Table 2: Upper and Lower Limits Imposed on the control surface

CONTROL VECTOR (Ū)	CONTROL SURFACE	LOWER LIMIT	UPPER LIMIT
U_1	AILERON	-20˚	20
U_2	ELEVATOR	-25˚	25˚
U_3	RUDDER	-25˚	25˚
U_4	THROTTLE	0	1

Modelling the Nondimensional Aerodynamic Force Coefficients in the Stability Frame

The equation defining aerodynamic forces and moments are determined by means of aerodynamic coefficient. The aerodynamic force coefficients were defined in stability reference frame (Fs). Some of the aerodynamic parameters were obtained from the conceptual manual and empirical data of the UAV category. This includes the dimensionless force coefficients given in Table 3.

Table 3: Aerodynamic Information

S/N	Aerodynamic Parameters	Values/Formulae
1	Maximum coefficient of Lift (C_L)	C_{LMax}=1.38
2	Maximum C_L angle ($c_{L\,max\,\alpha}$)	14.3˚
3	Zero lift angle	-3.6 ˚
4	Angle of twist	0
5	Drag polar for cruise condition	C_D=0.0109+0.0446C_L^2
6	Coefficient of side force	C_Y=−0.83β+0.1914U_3

The aerodynamic forces coefficient acting in the stability frame is as defined in equation 4

$$C_{F_{ac}}^{b} = \begin{bmatrix} -C_D \\ C_Y \\ -C_L \end{bmatrix}^{S} \quad \text{.....(4)}$$

$C_{F_{ac}}^{b}$ represent the nondimensional aerodynamic coefficient force from stability frame to body frame. C_D is the Coefficient of Drag Force, C_Y is the Coefficient of Side Force and C_L is Coefficient of Lift Force. The superscript s shows that the representation is in stability frame.

Dimensionalization of Aerodynamic Forces in the Body Frame

To dimensionalize equation 4, multiply it by the aircraft planform area (S) and the dynamic pressure (Q) to obtain the aerodynamic forces in the stability frame as shown in equation 5.

$$F^S = \begin{bmatrix} -F_D \\ F_Y \\ -F_L \end{bmatrix}^{S} = \begin{bmatrix} -C_D \cdot Q \cdot S \\ c_Y \cdot Q \cdot S \\ -C_L \cdot Q \cdot S \end{bmatrix}^{S} \quad \text{.....(5)}$$

Since the modelling was done in the body frame, equation 5 was rotated from the stability frame to the body frame using the appropriate rotation matrix, $T_{b/_S}(\alpha)$ as shown in equation 6.

$$T_{b/_S}(\alpha) = \begin{bmatrix} \cos\alpha & 0 & -\sin\alpha \\ 0 & 1 & 0 \\ \sin\alpha & 0 & \cos\alpha \end{bmatrix} \text{.....(6)}$$

Therefore, the aerodynamic force in the body frame is defined as:

$$F^b = T_{b/_S}(\alpha) \cdot F^s \text{.....(7)}$$

$$\mathrm{F^b} = \begin{bmatrix} \cos\alpha & 0 & -\sin\alpha \\ 0 & 1 & 0 \\ \sin\alpha & 0 & \cos\alpha \end{bmatrix} \begin{bmatrix} -\mathrm{C_D} \cdot \mathrm{Q} \cdot \mathrm{S} \\ \mathrm{c_Y} \cdot \mathrm{Q} \cdot \mathrm{S} \\ -\mathrm{C_L} \cdot \mathrm{Q} \cdot \mathrm{S} \end{bmatrix}^{\mathrm{S}} \text{.....(8)}$$

Modelling the Nondimensional Aerodynamic Moment Coefficients about Aerodynamic Center in the Body Frame

The modelling approach used in deriving the Nondimensional Aerodynamic Moment Coefficient equations for RCAM model design was adopted (Varga et al., 1997). The pitch, roll and yaw moment coefficients about the aerodynamic center in the body frame are defined as in equation

$$C^b_{M_{ac}} = \begin{bmatrix} C_{Lac} \\ C_{Mac} \\ C_{Nac} \end{bmatrix}^b = \eta + \frac{\partial C_m}{\partial X} + \omega^b_{b/_e} + \frac{\partial C_m}{\partial U} \begin{bmatrix} u_1 \\ u_2 \\ u_3 \end{bmatrix} \text{.....(9)}$$

where, η = Static moment effect

$\frac{\partial C_m}{\partial X}$ = Dynamic angular rate behavior matrix, which indicates the effect of the angular rates on the

moments.

$\frac{\partial C_m}{\partial U}$ = The matrix that captures the influence of the control inputs on the moments of the aircraft.

Dimensionalization of Aerodynamic Moments about Aerodynamic Center in the Body Frame

To dimensionalize equation 3.9, multiply it by the aircraft planform area (S), the dynamic pressure (Q) and the mean aerodynamic chord ($\bar{C}$) of the aircraft to obtain the aerodynamic moment in the body frame as shown in equation 3.10.

$$M^b_{Aac} = \bar{C}^b_{M_{ac}} QS\bar{C} \text{.....(10)}$$

Determination of Aerodynamic Moments about Center of Gravity in the Body Frame

The aerodynamic moment about the center of gravity was calculated using equation 11

$$M_{ACG}^{b} = M_{Aac}^{b} + F_{A}^{b} * (r_{CG}^{b} - r_{ac}^{b}) \quad \text{.....(11)}$$

Where, M_{Aac}^{b} is the dimensionalised aerodynamic moment about the aerodynamic center in the body frame.

F_{A}^{b} is the dimensionalised aerodynamic force in the body frame.

r_{cG}^{b} is the position of the CG

r_{ac}^{b} is the position of the aerodynamic center

$$r_{CG}^{b} = \begin{bmatrix} X_{cg} \\ Y_{cg} \\ Z_{cg} \end{bmatrix} \quad \text{.....(12)}$$

$$r_{ac}^{b} = \begin{bmatrix} X_{ac} \\ Y_{ac} \\ Z_{ac} \end{bmatrix} \text{.....(13)}$$

Where, X_{cg} is the position of CG along the x axis.

Y_{cg} is the position of CG along the y axis.

Z_{cg} is the position of CG along the z axis.

X_{ac} is the position of Aerodynamic center along the x axis.

Y_{ac} is the position Aerodynamic center along the y axis.

Z_{ac} is the position Aerodynamic center along the z axis.

Modelling the Propulsion effect

The hybrid energy-harvesting UAV is powered by fuel-cell. The thrust force due to the fuel-cell has only a component in the X-axis. This is because the cells are located parallel to the x-y plane of the aircraft. If the fuel-cells produce a thrust force denoted as $F_{1,}$ then F_1, is as expressed in equation

$$F_1 = U_4.mg \quad \text{.....(14)}$$

Where U4 represent the throttle control, m is the mass of the aircraft and g is the gravitational force. The contribution of the force generated by the engine (fuel-cell) to the forces acting on the aircraft is depicted in equation

$$F_{E}^{b} = \begin{bmatrix} F_1 \\ 0 \\ 0 \end{bmatrix}^{b} \text{.....(15)}$$

The moment generated by the engine about the center of gravity was computed with equation

$$M_{ECG}^{b} = \Delta t^{b} \cdot F_{E}^{b} \quad \text{.....(16)}$$

Δt^b is the distance between CG and position of the engine.

$$\Delta t^b = \begin{bmatrix} X_{cg} - X_{apt} \\ Y_{apt} - Y_{cg} \\ Z_{cg} - Z_{apt} \end{bmatrix} \quad \text{.....(17)}$$

X_{apt} is the position of the engine along the x axis

Y_{apt} is the position of the engine along the y axis

Z_{apt} is the position of the engine along the z axis

Therefore, moment generated by the engine about the center of gravity in the body frame is defined as;

Modelling the Gravity Effect

The gravitational force which is an external force that has components acting along the body axis was considered in the modelling of the aircraft. The force of gravity acts on the aircraft through the center of gravity of the aircraft and it is defined as;

The force due to gravity,

$$F_g = m.g \quad \text{.....(18)}$$

The force of gravity acting on the aircraft in the earth frame

$$F_g^e = m\begin{bmatrix} 0 \\ 0 \\ g \end{bmatrix}^e \quad \text{..... (19)}$$

Rotate equation 19 from earth to body frame using equation 20.

$$F_g^b = T_{b/e}(\phi, \theta, \psi) * F_g^e \quad \text{..... (20)}$$

$$F_g^b = \mathrm{m}\begin{bmatrix} -g sin X_8 \\ g cos X_8 sin X_7 \\ g cos X_8 sin X_7 \end{bmatrix} \quad \text{..... (21)}$$

The gravitational force creates zero moment about all the axes due to the body frame fixed to the center of gravity of the aircraft. Therefore, Gravitational moment,

$$M_g^b = \begin{bmatrix} Lg \\ Mg \\ Ng \end{bmatrix} = \begin{bmatrix} 0 \\ 0 \\ 0 \end{bmatrix} \quad \text{..... (22)}$$

Representation of Model in Explicit First-order Form

The aircraft model was finally, represented in explicit first order form using the computed moments and forces acting on the aircraft. The kinematical model was represented using Euler angle parameterization. The explicit first order form of the 12 states are given by 23 -28.

$$\begin{bmatrix} \dot{x}_1 \\ \dot{x}_2 \\ \dot{x}_3 \end{bmatrix} = \frac{1}{m} F^b - \omega_{b/e} \times V^b \quad \text{..... (23)}$$

where,

$$F^b = F_A^b + F_E^b + F_g^b \text{..... (24)}$$

$$\begin{bmatrix} \dot{x}_4 \\ \dot{x}_5 \\ \dot{x}_6 \end{bmatrix} = I_b^{-1} \left(M_{CG}^b - \omega_{b/e}^b X I_b \omega_{b/e}^b \right) \text{..... (25)}$$

where,

$$M_{CG}^b = M_{ACG}^b + M_{ECG}^b \text{..... (26)}$$

$$\begin{bmatrix} \dot{x}_7 \\ \dot{x}_8 \\ \dot{x}_9 \end{bmatrix} = \begin{bmatrix} 1 & \sin\emptyset \tan\theta & \cos\emptyset \tan\theta \\ 0 & \cos\emptyset & -\sin\emptyset \\ 0 & \sin\emptyset / \cos\theta & \cos\phi / \cos\theta \end{bmatrix} \begin{bmatrix} x_4 \\ x_5 \\ x_6 \end{bmatrix}^{\mathrm{b}} \text{.....(27)}$$

$$\begin{bmatrix} \dot{x}_{10} \\ \dot{x}_{11} \\ \dot{x}_{12} \end{bmatrix} = T_{e/b} \begin{bmatrix} x_1 \\ x_2 \\ x_3 \end{bmatrix}^{\mathrm{b}} \text{..... (28)}$$

$T_{e/b}$ is the transformation matrix from body to earth frame.

Trimming, Linearization and Decoupling of the Coupled Nonlinear Model

The 12 nonlinear equations of motion that describe the kinematics and dynamics of HEHU model were defined in equations 23 -28 in explicit first-order form. These equations represent the behavior of the HEHU. However, due to their complexity, they are difficult to use in designing controllers that would stabilize and improve the response of an aircraft. Therefore, it is paramount to decouple and linearize the nonlinear equations to develop the state space or transfer function models, which are simpler and compatible for designing aircraft control loops. The linearized model gives an approximate representation of the aircraft under specified conditions known as trim point. The linearized model differs from one operation condition to

another and it would only accurately represent the aircraft if it is operated within the vicinity of the operating point.

Trim

The trim conditions of a flight operation that is required to be linearized are based on the behavior of the states and inputs during the operation. The orientation of the aircraft is said to be trimmed at a set of constant controls. Under this condition, there should be no net forces or moments acting on the center of mass of the aircraft. For a nonlinear system given by

$$\dot{x}=f\ (x,\ u) \quad \text{..... (29)}$$

where, x is the system state and u is the input control, the system is said to be in equilibrium if:

$$f\ (x*,\ u*) = 0 \quad \text{..... (30)}$$

where, $x*$ and $u*$ are the equilibrium or trim point. Trim point can be steady state level flight, climbing, descending or constant turning. The trimming was done at steady state straight and level flight since that is the most important and prolonged flight phase. For the steady state straight and level flight, HEHU has the following flight conditions;

$$X= [20\ 0\ 0\ 0\ 0\ 0\ 0\ 0\ 0\ 0\ 0\ 0\ 100] \quad \text{..... (31)}$$

$$U= [0\ 0\ 0\ 0\ 0.1] \quad \text{..... (32)}$$

The MATLAB's *Trim* command was used for trimming by applying algorithm HEHU trim.m on the nonlinear model of the HEHU, and it solved equation 33 with the conditions given to provide the trimming points for the straight and level flight, which are represented by equations 34 and 35.

$$X_* = [105.643,\ 1.097,\ -2.897,\ -4.835e\text{-}22,\ -5.868e\text{-}21;$$
$$-1.788e\text{-}21,\ 0.357,\ -0.022,\ –3.729e\text{-}14,\ 8.424e\text{-}12,\ 0,\ -100] \quad \text{..... (33)}$$

$$U_*= [-0.018\ -0.272\ 0.019\ 0.772] \quad \text{..... (34)}$$

Decoupling and Linearization

The short-term local behavior of the HEHU at a given flight condition can be approximated by the linearization of its nonlinear model about the equilibrium points obtained by trimming. Before linearization, the system states and control inputs are decoupled into lateral and longitudinal modes. To obtain the lateral model of the HEHU, the longitudinal states; u, w, θ and q are equated to zero. The lateral control inputs are U_1 and U_3. For the longitudinal motion model, the lateral states; v, ϕ, ψ, p, and r were equated to zero. The longitudinal control inputs are U_2 and U_4

The general state space model for a linear differential system is given by;

$$\dot{x}=Ax+Bu \quad \text{..... (35)}$$

$$y = Cx + Du \quad \text{..... (36)}$$

Where A, B, C and D the constant matrices. A is (n x n) system matrix, B is the (n x p) control matrix representing the relationship between the control inputs and states. C is the (q x n) output matrix representing the relationship between states and the outputs and D is a (q x p) representing the relationship between control inputs and outputs.

The trim point obtained in equation 33 can be used to linearize the system with the aid of Taylor series expansion method. The approximate linear model after applying Taylor series expansion method is given as;

$$\tilde{\dot{x}} = \frac{\partial f(x^*,u^*)}{\partial x}\tilde{x} + \frac{\partial f(x^*,u^*)}{\partial u}\tilde{u} \quad \text{..... (37)}$$

$$\tilde{y} = \frac{\partial h(x^*,u^*)}{\partial x}\tilde{x} + \frac{\partial h(x^*,u^*)}{\partial u}\tilde{u} \quad \text{.....(38)}$$

where, $\frac{\partial f(x^*,u^*)}{\partial x}$, $\frac{\partial f(x^*,u^*)}{\partial u}$, $\frac{\partial h(x^*,u^*)}{\partial x}$ and $\frac{\partial h(x^*,u^*)}{\partial u}$ are Jacobian matrices. Comparing equations 35 and 36 with equations 37 and 38, A = $\frac{\partial f(x^*,u^*)}{\partial x}$, B = $\frac{\partial f(x^*,u^*)}{\partial u}$, C = $\frac{\partial h(x^*,u^*)}{\partial x}$ and D = $\frac{\partial h(x^*,u^*)}{\partial u}$.

However, the linear models for this thesis were obtained by using the *linmod* MATLAB command without solving the Jacobian matrices. The nonlinear model of the aircraft was linearized about the trim condition obtained at previous step of the algorithm HEHUtrim.m. The extraction of the state space model was executed by linearization step of the developed algorithm Linearized_model_ALTA_MODEL.m. The details of the algorithm are explained in Appendix C.

The lateral state space and control matrices are given by

A_lat =

$$\begin{matrix} -4.8190 & -16.3260 & -92.4028 & 8.9137 & 0 & 0 \\ -0.0507 & -0.0930 & 0.0404 & 0 & 0 & 0 \\ 0.0237 & 0.0038 & -0.0382 & 0 & 0 & 0 \\ 0 & 1.0000 & 0.1411 & 0 & 0 & 0 \\ 0 & 0 & 0.9300 & 0 & 0 & 0 \\ 0.9193 & 0 & 0 & 14.108 & 93.4846 & 0 \end{matrix}$$

B_lat =

$$\begin{matrix} 0 & 104.2885 \\ -1.9753 & 0.7424 \\ -1.9753 & 0.7424 \\ -0.0414 & -0.8431 \\ 0 & 0 \\ 0 & 0 \\ 0 & 0 \end{matrix}$$

C_lat =

$$\begin{matrix} 1 & 0 & 0 & 0 & 0 & 0 \\ 0 & 1 & 0 & 0 & 0 & 0 \\ 0 & 0 & 1 & 0 & 0 & 0 \\ 0 & 0 & 0 & 1 & 0 & 0 \\ 0 & 0 & 0 & 0 & 1 & 0 \\ 0 & 0 & 0 & 0 & 0 & 1 \end{matrix}$$

D_lat =

$$\begin{matrix} 0 & 0 \\ 0 & 0 \\ 0 & 0 \\ 0 & 0 \\ 0 & 0 \\ 0 & 0 \end{matrix}$$

The longitudinal state space and control matrices are given by

A_lon =

$$\begin{matrix} -1.1728 & -5.7056 & 15.7084 & -9.6965 & 0 & 0 \\ -5.9728 & -32.7138 & 88.9408 & 1.3680 & 0 & 0 \\ -0.0076 & -0.0427 & -0.0646 & 0 & 0 & 0 \\ 0 & 0 & 0.9193 & 0 & 0 & 0 \\ 0.9884 & -0.1394 & 0 & -0.0000 & 0 & 0 \\ 0.1517 & 0.9086 & 0 & -93.4846 & 0 & 0 \end{matrix}$$

B_lon =

$$\begin{matrix} -38.6557 & 9.8100 \\ -216.6939 & 0 \\ -4.0425 & 0.0037 \\ 0 & 0 \\ 0 & 0 \\ 0 & 0 \\ 0 & 0 \end{matrix}$$

C_lon =

$$\begin{matrix} 1 & 0 & 0 & 0 & 0 & 0 \\ 0 & 1 & 0 & 0 & 0 & 0 \\ 0 & 0 & 1 & 0 & 0 & 0 \\ 0 & 0 & 0 & 1 & 0 & 0 \\ 0 & 0 & 0 & 0 & 1 & 0 \\ 0 & 0 & 0 & 0 & 0 & 1 \end{matrix}$$

D_lon=

$$\begin{matrix} 0 & 0 \\ 0 & 0 \\ 0 & 0 \\ 0 & 0 \\ 0 & 0 \\ 0 & 0 \end{matrix}$$

Flight Control Loops

Flight control system design is complicated by the problem of external disturbance, uncertain measurements and modeling uncertainties which affects the stability of the aircraft [44]. To resolve the flight stability issues, a control algorithm must be applied to the aircraft model. Linear Quadratic Controller (LQR) was employed in this thesis. LQR was chosen because it is a multiple input multiple output controller, robustness, good stability margin and its ability to overcome huge disturbances without reducing working performance [37]. Hence LQR provides better disturbance rejection and overall performance when compared to PID controllers.

Both the lateral and longitudinal control loops utilizing LQR were developed using linear system models. Given the perturbation linear model in a general state space as;

$$\tilde{x}=A\tilde{x}+B\tilde{u} \quad \text{.....39}$$

$$\tilde{y} = C\tilde{x}+D\tilde{u} \quad \text{.....40}$$

Where the $\tilde{x}$ = $x-x_n$, $\tilde{u}$ = $u-u_n$ and $\tilde{y}=y-y_n$ are the perturbed states, control inputs and outputs around the trim states x_n, control inputs u_n and outputs y_n respectively. $\tilde{x}$ and $\tilde{u}$ are the errors between the actual states and control values, and controlled values at the commanded trim point. Since the objective is to drive $\tilde{x}$ and $\tilde{u}$ to zero, it necessary to determine the optimal gain matrix, K_{lqr} with state feedback law given as;

$$\tilde{u} = K_{lqr}\tilde{x} \quad \text{.....41}$$

By driving the errors to zero minimizes the performance index (Quadratic cost function), which is given as;

$$J = \int_0^{\infty} (x(t)^T Qx(t) + u(t)^T Ru(t))dt \quad \text{.....42}$$

With equation 42 subjected to the system dynamics represented by equation 39, where Q is a positive semi-definite symmetric weighing matrix, Q≥0; and R is a positive definite symmetric weighing matrix R>0. The amount of perturbation control $\tilde{u}(t)$ used is affected by the value of R and the perturbation system response is affected by the values of the elements of Q, $\tilde{x}(t)$. K_{lqr} is obtained by

$$K_{lqr} = K = R^{-1}B^TS \quad \text{.....43}$$

S is the unique positive semi-definite and symmetric solution to the Algebraic Reccati Equation (ARE). S is computed by solving the reduced matrix Riccati equation in equation 3.45 for Q and R weighting matrices.

$$A^T S + SA + Q - SBR^{-1} B^T S = 0 \quad \text{.....44}$$

MATLAB function LQR was used to determine the K_{lqr} gain matrix. The weighting matrix Q_{long} and R_{long} in the longitudinal motion of the HEHU is as follow;

Q_{long} =

$$\begin{matrix} 1 & 0 & 0 & 0 & 0 & 0 \\ 0 & 1 & 0 & 0 & 0 & 0 \\ 0 & 0 & 1 & 0 & 0 & 0 \\ 0 & 0 & 0 & 1 & 0 & 0 \\ 0 & 0 & 0 & 0 & 1 & 0 \\ 0 & 0 & 0 & 0 & 0 & 1 \end{matrix}$$

R_{long} =

$$\begin{matrix} 1 & 0 & 0 \\ 0 & 1 & 0 \\ 0 & 0 & 1 \end{matrix}$$

The weighting matrix Q_{lat} and R_{lat} in the lateral motion of the HEHU is as follow;

Q_{lat} =

$$\begin{matrix} 1 & 0 & 0 & 0 & 0 & 0 \\ 1 & 1 & 0 & 0 & 0 & 0 \\ 0 & 0 & 1 & 0 & 0 & 0 \\ 0 & 0 & 0 & 1 & 0 & 0 \\ 1 & 0 & 0 & 0 & 1 & 0 \\ 1 & 0 & 0 & 0 & 0 & 1 \end{matrix}$$

R_{lat} =

$$\begin{matrix} 1 & 0 & 0 \\ 0 & 1 & 0 \\ 0 & 0 & 1 \end{matrix}$$

RESULTS AND DISCUSSION

In this section, the results obtained from the designed 6DOF model, linearized models and the control loops of the HEHU are discussed.

Nonlinear Coupled 6DOF HEHU Model Results

After the modelling of the UAV by considering the 12 state inputs and four controls (aileron u1, elevator u2, rudder u3 and throttle u4) to depict the behavior of the UAV, it was coded and simulated in the MATLAB/Simulink platform to observe its stability and accuracy. The Nonlinear coupled 6DOF HEHU model's MATLAB block diagram is as shown in Figure 2.

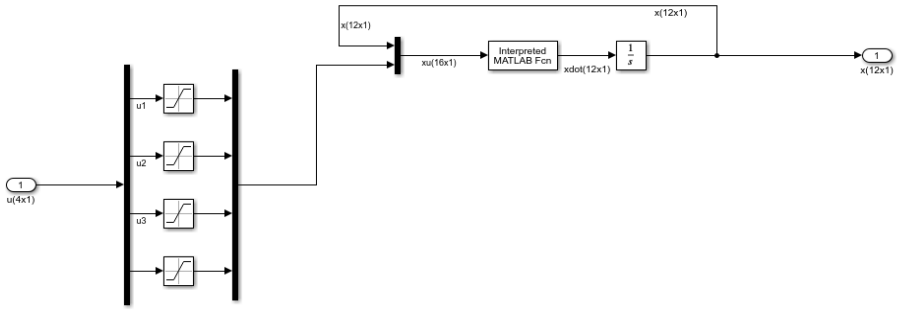

Figure 2: Nonlinear Coupled 6DOF HEHU Model

The model was then initialized with state input and control input defined in equation 45 and 46 respectively,

x0= [20 0 0 0 0 0 0 0.1 0 0 0 -3000] 45

u= [0 -0.1 0 0.1] 46

The model was run for 180 seconds to observe its accuracy and stability within two different simulating environments. The first environment was to observe the accuracy of the model by deflecting the elevator, u2 down to pitch up the aircraft, while moving forward and the results were plotted. Figure 3 shows the output of the input controls with a constant throttle and elevator deflection. (No aileron, rudder and constant throttle).Figure4 shows the output of the state inputs when the UAV was pitched up, it could be observed from the figure that states related to the forward movement and ascent of the aircraft, such as forward velocity, pitch angle and pitch rate, corresponds well to the input given. However, all the roll and yaw angles/rates remained unchanged. There was no side velocity (0 m/s), p (roll rate, x4), q (yaw rate, x6), roll angle, and yaw angle.

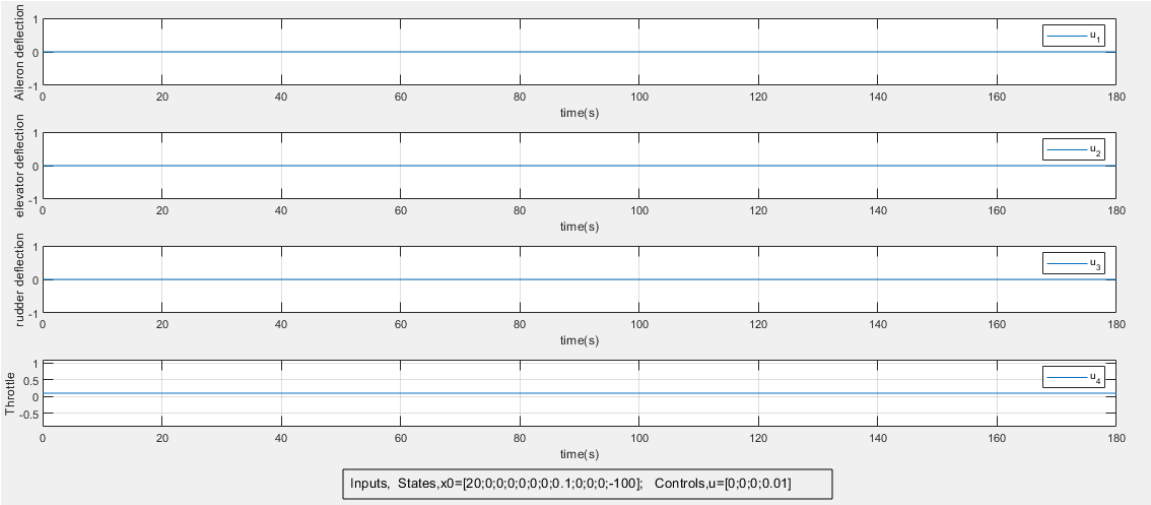

Figure 3: Graph of Controls without Perturbation

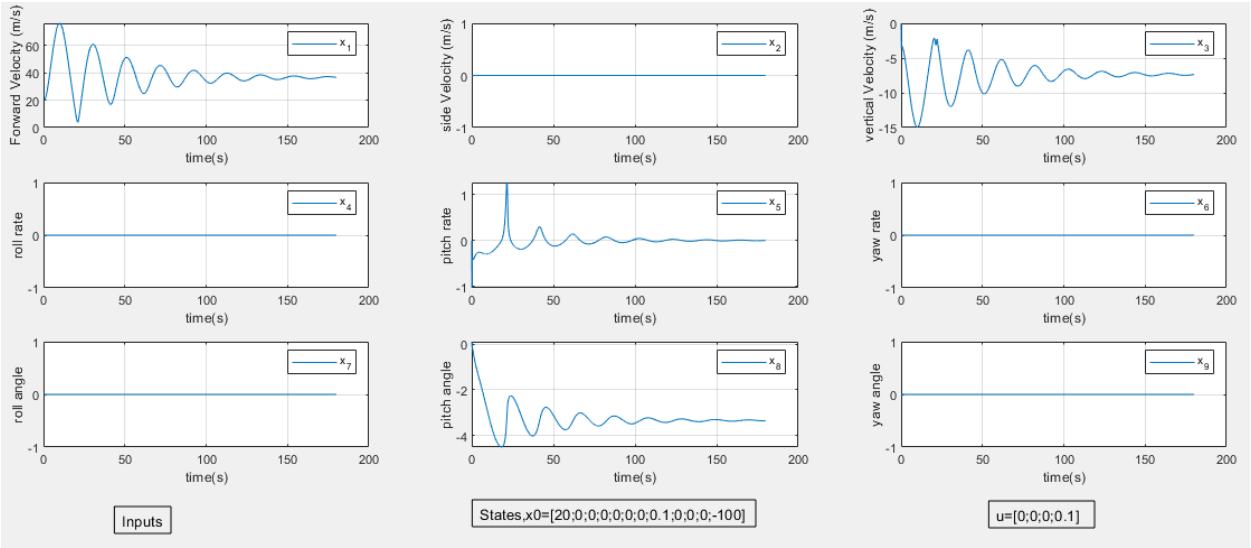

Figure 4: Graph of State Inputs

The stability of the model was examined by perturbing the aircraft at some instances of its operation to observe whether it would recover from the perturbations. The UAV whilst cruising, with the other control inputs (u2, u3 and u4) remained unchanged, the UAV was rolled by deflect the aileron at an angle of 5 degrees at 30 seconds. The deflection was held for 5 seconds and then removed at 35s to observe the response of the UAV as depicted in Figure 5. From Figure 6, it could be observed that at 30 seconds all the states such as the side velocity, roll rate/angle and yaw rate/angle that are related to the rolling motion of UAV were affected by the aileron deflection.

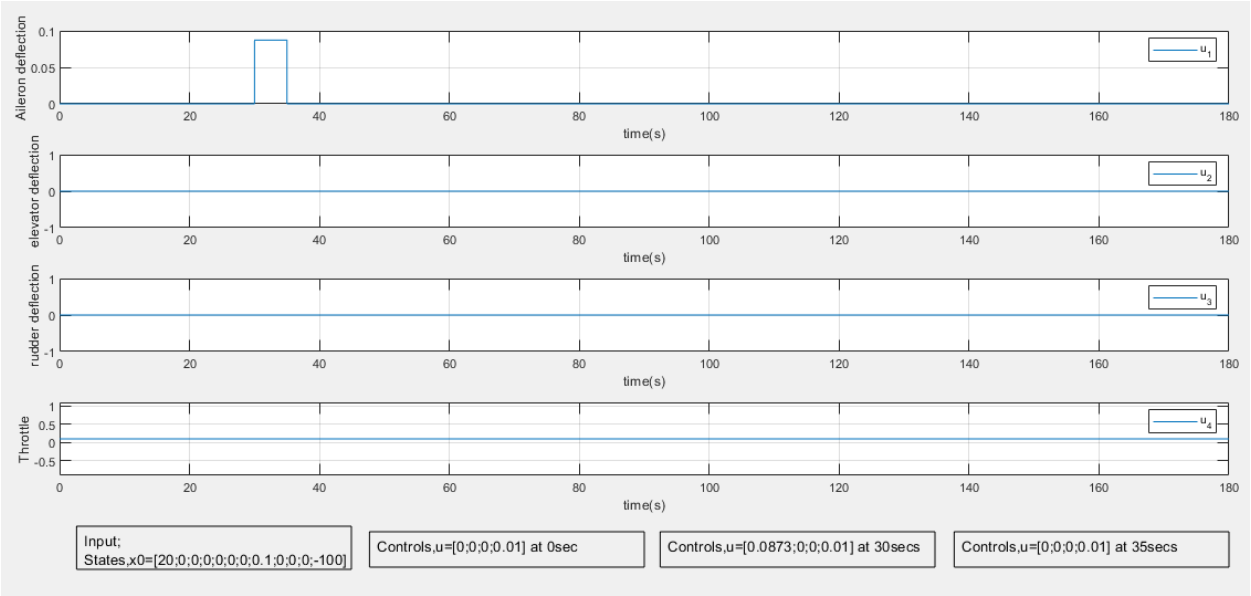

Figure 5: Graph of Controls with Perturbation

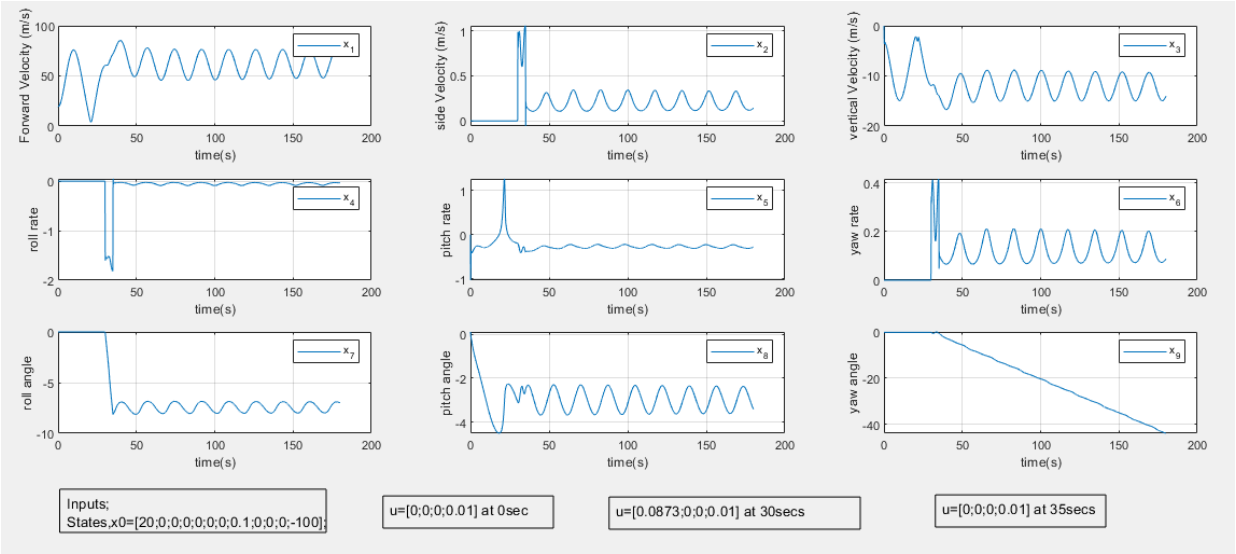

Figure 6: Graph of State Inputs after Perturbation

However, at 35s (when the deflection was removed), most of the states did not return back to their original states. Therefore, a control system was designed to stabilize and control the model. Before designing the control system, the 6DOF nonlinear HEHU equations was linearized and decoupled into longitudinal motion and lateral motion.

Linearized Model Results

After linearization, the accuracy of the linearized model; both lateral and longitudinal motion models was tested by simulating the models with appropriate control inputs and the results were plotted. The accuracy of the lateral model was tested by deflecting the ailerons and rudder, at

different instances. The ailerons were deflected at 50s, and the deflections were removed at 70s. On the other hand, the rudder was deflected at 80s, and the deflections were removed at 120s. In all cases, the lateral states of the aircraft corresponded accurately to the deflections as depicted in Figure 7.

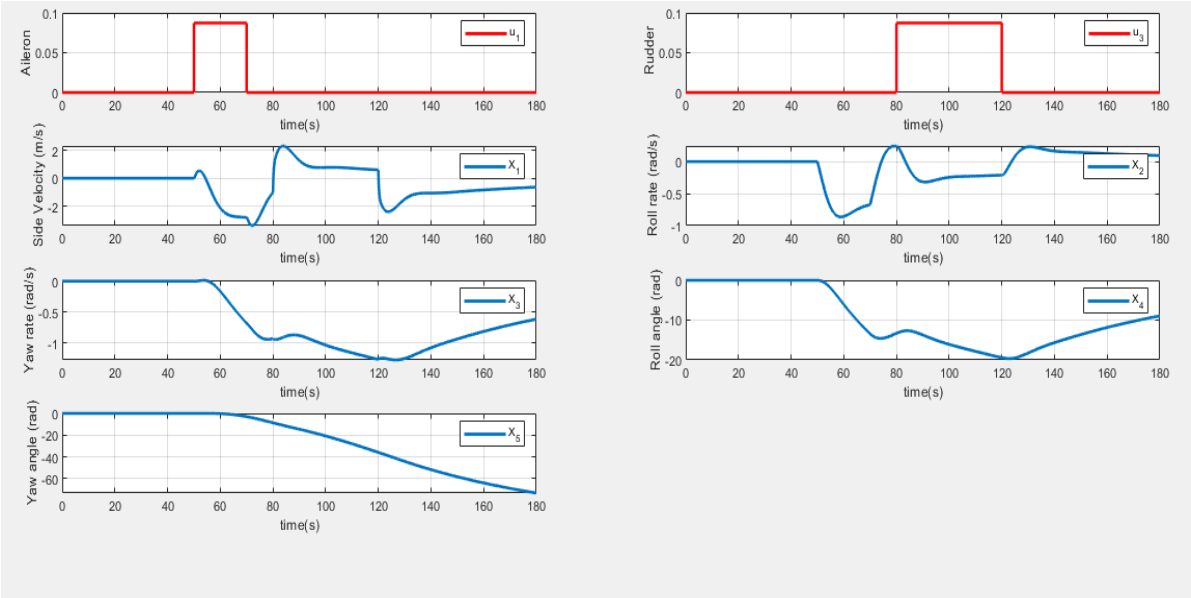

Figure 7: Lateral Motion Model

In Figure 8, the elevators were then deflected at 50s to increase the rate at which the pitching occurs. The deflections were removed at 80s. The longitudinal states of the aircraft corresponded accurately to the deflections. These results showed that the longitudinal and lateral models of the aircraft accurately depict its motion.

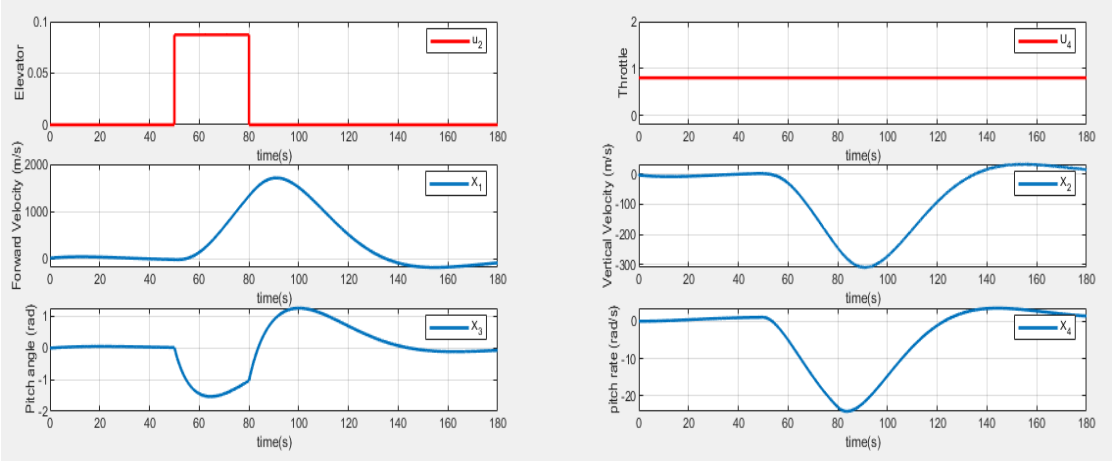

Figure 8: Longitudinal Motion Model

Autopilot Control Loops Design

Fig 9 and 10 depict the control loop for longitudinal and lateral model respectively using Linear Quadratic Regulator.

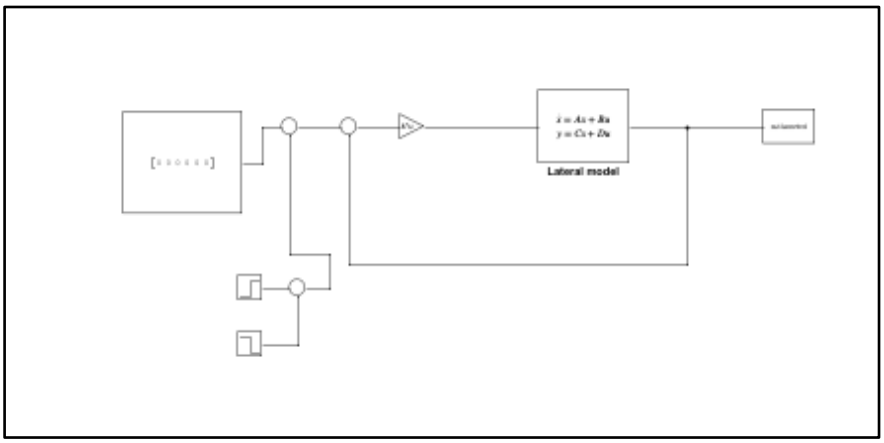

Figure 9 Lateral Control Loop

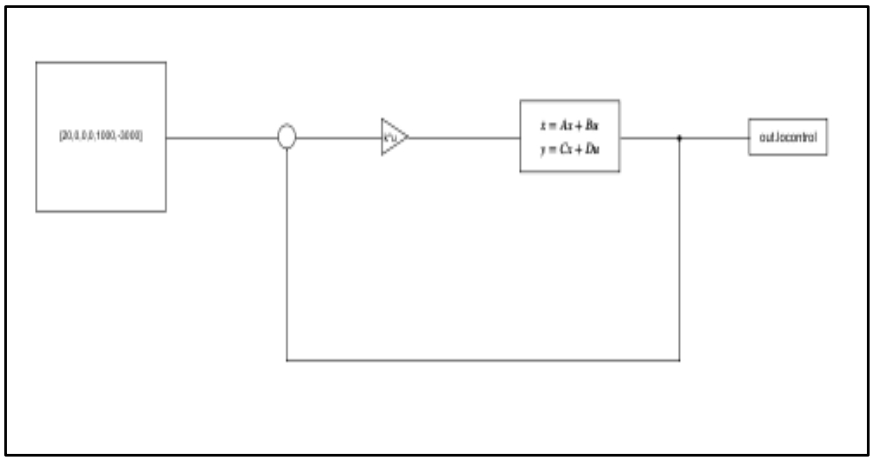

Figure 10 Longitudinal Control Loop

In order to test the stability of the Lateral control loop, with lateral states initially at zero, disturbances were injected to the system at 3s and removed at 5s. In Figure 11 it was observed that the control system was able to recover from the perturbations and stabilize the affected states of the system. Figure 12 also depicts the outcome of the longitudinal control loop. It was observed that all the longitudinal states were able to stabilize.

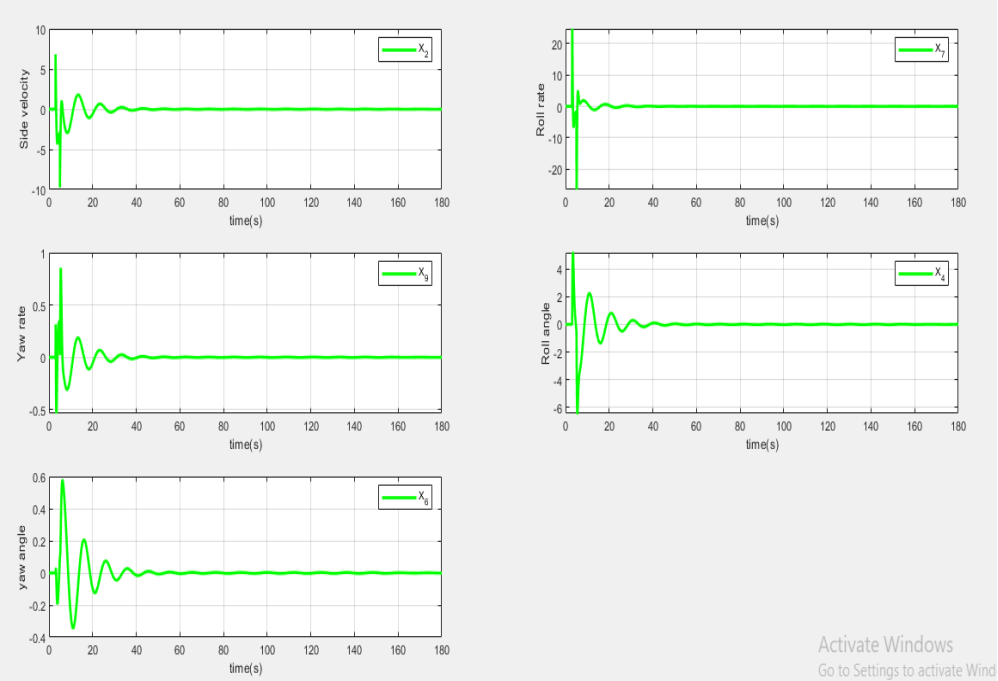

Figure 11 Graph of Lateral Control Loop

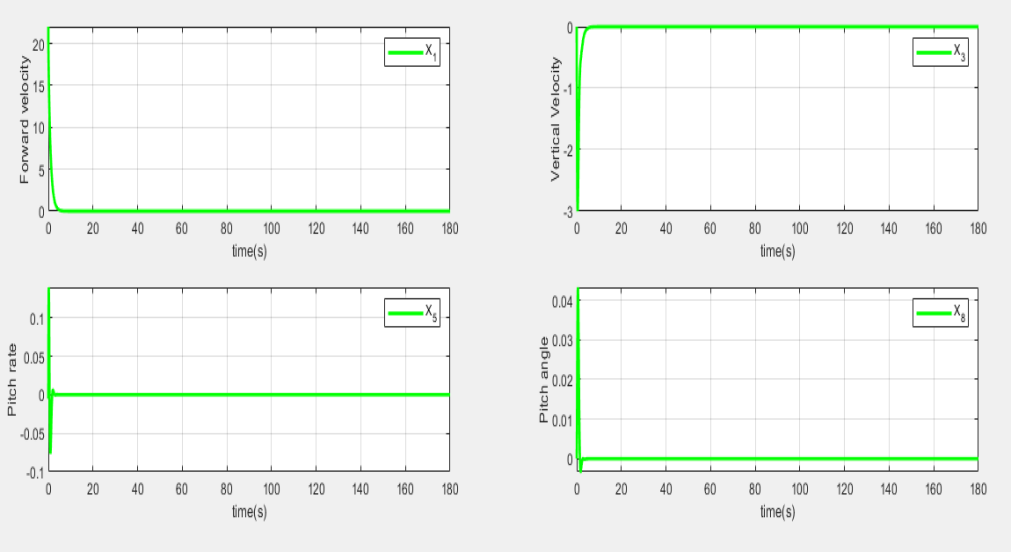

Figure 12 Graph of Longitudinal Control Loop

CONCLUSION

The development of a nonlinear simulation model for the energy-harvesting UAV was conducted within the MATLAB/Simulink environment, has significantly contributed to understanding its dynamics and behavior. This model, incorporating aerodynamic components in the 6DOF equation of motion, propulsion, and gravity effects, underwent trimming, decoupling, and linearization processes to enhance its accuracy and applicability. The open-loop

responses of the models to various control inputs have demonstrated their precision in representing the UAV's behavior. Utilizing the linearized models, an autopilot system was designed to stabilize the UAV, even in the presence of uncertainty. The robustness of the LQR-based autopilot has been highlighted, showing its capability to ensure safe flight amidst disturbances and uncertainties.Furthermore, the trimming of the developed nonlinear model using MATLAB's trim function, followed by decoupling and linearization, facilitated the design of control loops. Employing LQR for control loop design proved advantageous due to its robustness, stability margin, and ability to handle significant disturbances without compromising performance. Testing the accuracy and stability of the control loops by introducing perturbations at different times revealed that the UAV maintained stability across all system states. This indicates the effectiveness of the control system in maintaining the UAV's desired trajectory and stability under varying conditions.

REFERENCES

Abubakar, U., Zaharuddeen, H., Umar, M., Shehu, A. M., & Momoh, M. O. (2019). Graphical User Interface (GUI) Based Position and Trajectory Tracking Control for the Ball and Plate System Using H-Infinity Controller. *Covenant Journal of Informatics and Communication Technology*, *5*(1).

Ahmed, A. E., Hafez, A., Ouda, A. N., Ahmed, H. E. H., & Abd-Elkader, H. M. (2015). Modeling of a small unmanned aerial vehicle. *Adv Robot Autom*, *4*(126), 2.

Akhtar, N., Whidborne, J., & Cooke, A. (2009). Wind shear energy extraction using dynamic soaring techniques. *47th AIAA Aerospace Sciences Meeting Including the New Horizons Forum and Aerospace Exposition*, 734.

Ashraf, A., Mei, W., Gaoyuan, L., Anjum, Z., & Kamal, M. M. (2018). Design linear feedback and LQR controller for lateral flight dynamics of F-16 aircraft. *2018 International Conference on Control, Automation and Information Sciences (ICCAIS)*, 367–371.

Balas, G. J. (2003). Flight control law design: An industry perspective. *European Journal of Control*, *9*(2–3), 207–226.

Boukoberine, M., & Zhou, Z. (2019). A critical review on unmanned aerial vehicles power supply and energy management: Solutions, strategies, and prospects. *Elsevier Applied Energy* , *255*, 113823. https://www.sciencedirect.com/science/article/pii/S0306261919315107

Chao, H., Cao, Y., & Chen, Y. (2007). Autopilots for small fixed-wing unmanned air vehicles: A survey. *2007 International Conference on Mechatronics and Automation*, 3144–3149.

Chaturvedi, S. K., Sekhar, R., Banerjee, S., & Kamal, H. (2019). Comparative review study of military and civilian unmanned aerial vehicles (UAVs). *INCAS Bulletin*, *11*(3), 181–182.

Escareno, J., Salazar-Cruz, S., & Lozano, R. (2006). Attitude stabilization of a convertible mini birotor. *2006 IEEE Conference on Computer Aided Control System Design, 2006 IEEE International Conference on Control Applications, 2006 IEEE International Symposium on Intelligent Control*, 2202–2206.

GARTEUR. (1995). *QART ## lR*.

Guo, Y., Luo, L., & Bao, C. (2022). Design of a Fixed-Wing UAV Controller Combined Fuzzy Adaptive Method and Sliding Mode Control. *Mathematical Problems in Engineering*, *2022*(1), 2812671.

Hamissi, A., Bouzid, Y., Dabouze, N., Zaouche, M., Busawon, K., & Hamerain, M. (2019). Combining homogeneous high order sliding mode and nonlinear dynamic inversion for fixed wing aircraft attitude and speed control. *IFAC-PapersOnLine*, *52*(12), 304–309.

Hussain, I., Awad, M. I., Junaid, A. Bin, Renda, F., Seneviratne, L., & Gan, D. (2018). Dynamic modeling and numerical simulations of a passive robotic walker using Euler-Lagrange method. *2018 11th International Symposium on Mechatronics and Its Applications (ISMA)*, 1–6.

Kanokmedhakul, Y., Pholdee, N., Bureerat, S., & Panagant, N. (2019). LQR Aircraft pitch controller design for handling disturbance using differential evolution. *Journal of Research and Applications in Mechanical Engineering*, *7*(2), 145–153.

Karakaş, D. (2007). *Nonlinear modeling and flight control system design of an unmanned aerial vehicle*. https://open.metu.edu.tr/handle/11511/17085

Karlsson, M. (2002). *Control of unmanned aerial vehicles using non-linear dynamic inversion*. Institutionen för systemteknik.

Khan, W., & Nahon, M. (2013). *Dynamics Modeling of a Highly-Maneuverable Fixed-Wing UAV*.

Kumar, Y. (2015). *Design of Autopilot for Unmanned Air Vehicle*. https://doi.org/10.13140/RG.2.1.2939.6963

Liu, M., Egan, G. K., & Santoso, F. (2015). Modeling, autopilot design, and field tuning of a UAV with minimum control surfaces. *IEEE Transactions on Control Systems Technology*, *23*(6), 2353–2360.

Martini, S., Sönmez, S., Rizzo, A., Stefanovic, M., Rutherford, M. J., & Valavanis, K. P. (2022). Euler-Lagrange modeling and control of quadrotor UAV with aerodynamic compensation. *2022 International Conference on Unmanned Aircraft Systems (ICUAS)*, 369–377.

Mazlan, N. E. A., Shamsudin, S. S., Pairan, M. F., Yaakub, M. F., & Ramli, M. F. (2021). The Design of an Automatic Flight Control System and Dynamic Simulation for Fixed-Wing Unmanned Aerial Vehicle (UAV) using X-Plane and LabVIEW. *Progress in Aerospace and Aviation Technology*, *1*(1). https://doi.org/10.30880/paat.2021.01.01.007

Mir, I., Eisa, S. A., Taha, H., Maqsood, A., Akhtar, S., & Islam, T. U. (2021). A stability perspective of bio-inspired UAVs performing dynamic soaring optimally. *Bioinspir. Biomim*, *16*.

Mohammed, A., Ibrahim, B. G., Momoh, M. O., Ter, K. P., Adetifa, A. O., & Oluwole, D. A. (2022). Challenges of Ground Control System in Ensuring Safe Flights for Unmanned Aerial Vehicles. *Mekatronika: Journal of Intelligent Manufacturing and Mechatronics*, *4*(1), 8–19.

Mohsan, S., Khan, M., Noor, F., & Ullah, I. (2022). Towards the unmanned aerial vehicles (UAVs): A comprehensive review. *Drones*, *6*(6), 147. https://www.mdpi.com/2504-446X/6/6/147

Momoh, M. O., Shobowale, K. O., Abubakar, Z. M., Yahaya, B., & Ibrahim, Y. (2022). *Blockchain Adoption in Aviation: Opportunities and Challenges*.

Momoh, M. O., Ubadike, O. C., Kachalla, I. A., Isa-Bello, M. A., Chinedu, P. U., & Abdullahi, M. B. (2021). VSS-LMS: LMS Algorithm Experimental Approach. *Mekatronika: Journal of Intelligent Manufacturing and Mechatronics*, *3*(2), 31–36.

Muraleedharan, N., Cohen, D. S., Estrela, V. V, Hemanth, J., Saotome, O., Nikolakopoulos, G., Sabatini, R., & Wackett, L. (2020). Modelling and simulation of UAV systems. *Imaging and Sensing for Unmanned Aircraft Systems*, *1*, 101–121.

Naser, E., Elmajdub, F., & Bhardwaj, A. (2016). To Design an Aircraft Control System. *Etd.Repository.Ugm.Ac.Id*, *11*(1), 36–63. https://etd.repository.ugm.ac.id/home/detail_pencarian_downloadfiles/1107557

Oktay, T., Konar, M., Onay, M., Aydin, M., & Mohamed, M. A. (2016). Simultaneous small UAV and autopilot system design. *Aircraft Engineering and Aerospace Technology*, *88*(6), 818–834.

Purnawan, H., & Purwanto, E. B. (2017). Design of linear quadratic regulator (LQR) control system for flight stability of LSU-05. *Journal of Physics: Conference Series*, *890*(1), 012056.

Qazi, A. I., Ahsan, M., Ashraf, Z., & Ahmad, U. (2017). Modeling of a UAV longitudinal dynamics through system identification technique. *International Journal of Aerospace and Mechanical Engineering*, *11*(8), 1518–1522.

Ryll, M., Bülthoff, H. H., & Giordano, P. R. (2014). A novel overactuated quadrotor unmanned aerial vehicle: Modeling, control, and experimental validation. *IEEE Transactions on Control Systems Technology*, *23*(2), 540–556.

Sachs, G. (2005). Minimum shear wind strength required for dynamic soaring of albatrosses. *Ibis*, *147*(1), 1–10.

Saeed, A. S., Younes, A. B., Islam, S., Dias, J., Seneviratne, L., & Cai, G. (2015). A review on the platform design, dynamic modeling and control of hybrid UAVs. *2015 International Conference on Unmanned Aircraft Systems (ICUAS)*, 806–815.

Salman, S. A., & Anavatti, S. G. (2012). Fuzzy model based control of unmanned aerial vehicle. *IFAC Proceedings Volumes*, *45*(1), 109–114.

Sanusi, S., Mohammed, A., Dandago, K. K., & Kadiri, M. (2022). *A Framework for the Development of an Autopilot System for Unmanned Aerial Vehicles*.

Simmons, B. (2018). *System identification of a nonlinear flight dynamics model for a small, fixed-wing UAV* [Virginia Tech]. https://vtechworks.lib.vt.edu/items/92d6ff12-706b-4879-bad4-9174b9a2dc90

Srour, A., Noura, H., & El Assaad, S. (2021). Modeling, design and manufacturing of delta-wing UAV. *2021 International Conference on Unmanned Aircraft Systems (ICUAS)*, 1573–1579.

Ubadike, O. C., Dandago, K. K., Zango, M. S., Mohammed, A., Okonkwo, P. P., Chollom, T. D., Muhammad, B. B., & Adeboye, C. O. (2022). Development of Flight Dynamics Model for AH-25 Hybrid Unmanned Aerial Vehicle. *Applications of Modelling and Simulation*, *6*, 49–63.

Ubadike, O., Udekwe, D., Bonet, M., Momoh, M., Makinde, O., Omada, J., & Mohammed, A. (2022). *DEVELOPMENT OF A BLDC MOTOR BASED STARTER-GENERATOR FOR AN EXPERIMENTAL UAV*. *7*, 932–937.

Varga, A., Looye, G., & Moormann, D. (1997). *ORIGINAL: ENGLISH GARTEUR/TP-088-36 April 4, 1997*.
https://citeseerx.ist.psu.edu/document?repid=rep1&type=pdf&doi=0553fc96f592c0bdbf169860cb7c921faf2073f9

Wahab, A. A., Mamat, R., & Shamsudin, S. S. (2006). The development of autopilot system for an autonomous UAV helicopter model. *1st Regional Conference on Vehicle Engineering & Technology*.

Wang, W., An, W., & Song, B. (2022). Modeling and application of dynamic soaring by unmanned aerial vehicle. *Applied Sciences*, *12*(11), 5411.

Yao, H., Qin, R., & Chen, X. (2019). Unmanned aerial vehicle for remote sensing applications—A review. *Remote Sensing*, *11*(12), 1443. https://www.mdpi.com/2072-4292/11/12/1443